

Cyclic simulation of Stirling cryocoolers

M.D. Atrey, S. L. Bapat and K.G. Narayankhedkar

Department of Mechanical Engineering, Indian Institute of Technology, Powai,
Bombay-400076, India

Received 12 October 1989

Analysis of Stirling cryocoolers has been an important research topic over the last 30 years. The actual and the ideal Stirling cycles are distinctly different and performance prediction of the actual cycle has been a subject of interest to scientists. In this paper cyclic simulation of the actual Stirling cycle cryocooler has been performed on the microcomputer. The results are compared with the actual measured results and they show better agreement than for existing analyses. The analysis has been further extended to fit different machines.

Keywords: cryocoolers; mathematical models; cooling systems

Nomenclature			
C	Heat capacity ($J g^{-1} K^{-1}$)	W_{CS}	Mass flow rate of gas in compression space ($g s^{-1}$)
C_C	Displacer gap thickness (m)	W_{ES}	Mass flow rate of gas in expansion space ($g s^{-1}$)
C_P	Compressor power input (W)	W_{RS}	Mass flow rate of gas in regenerator ($g s^{-1}$)
C_{PL}	Loss due to pressure drop (W)		
C_{PM}	Heat capacity of regenerator matrix ($J g^{-1} K^{-1}$)	<i>Subscripts</i>	
D_{RMT}	Temperature swing for regenerator material (K)	avg	Average
D_P	Diameter of piston (m)	C	Compression space
E	Efficiency of regenerator	CC	Compression clearance
F	Fraction of gas inventory	CM	Maximum compression space
K	Swept volume ratio of compression and expansion spaces	D	Dead
K_g	Thermal conductivity ($W m^{-1} K^{-1}$)	DC	Cooler dead space
L_D	Length of displacer (m)	DCD	Condenser dead space
M	Moles of gas	E	Expansion space
M_{MX}	Mass of matrix material (kg)	EC	Expansion clearance
M_w	Molecular weight (g)	EM	Maximum expansion space
N_U	Speed ($rev s^{-1}$)	m	Mean
P	Pressure (bar)	MAX	maximum
Q_I	Ideal refrigeration effect (W)	MIN	Minimum
Q_{IP}	Refrigeration effect considering pressure drop (W)	p	Constant pressure
Q_{PU}	Pumping loss (W)	RD	Regenerator dead space
Q_R	Loss due to regenerator ineffectiveness (W)	T	Total
Q_S	Loss due to shuttle heat conduction (W)	v	Constant volume
Q_{TS}	Loss due to temperature swing (W)		
R	Universal gas constant ($J g^{-1} mol^{-1} K^{-1}$)	<i>Greek symbols</i>	
S_D	Stroke of displacer (m)	α	Phase difference between displacer and piston
T	Temperature (K)	γ	Ratio of specific heat capacities
V	Volume (m^3)	Δ	Small difference
		ϕ	Crank angle

The ideal Stirling cycle has two isothermal processes, i.e. isothermal compression and isothermal expansion, and two constant volume processes, i.e. heat addition and heat rejection. Schmidt¹ presented an analysis for the ideal Stirling cycle. Martini² further analysed the cycle for realistic losses, keeping the basic assumptions the

same. Recently, Walker *et al.*³ have applied Martini's analysis to PPG-102 and compared the experimental and analytical results.

In practice, the process of compression always tends to be adiabatic, as it is impossible to obtain an isothermal compression process. The adiabatic compression process

can be seen as covering the cylinder jacket by an insulation which prevents any heat leakage to or from the surroundings. The cooling of the gas in the after-cooler helps to bring down the discharge temperature. The expansion process, on the other hand, is one which tends towards lowering of the temperature and pressure. But, at the same time, there is an inflow of heat from the gas which is cooled/liquefied on the condenser. This tends to increase the temperature of the working fluid which would otherwise have decreased. As a result, the temperature of the gas remains more or less constant, making the process of expansion almost isothermal. Thus, the compression process tends towards being adiabatic and the expansion process towards being isothermal.

Analysis

Features of the approach

Martini's analysis² considers dead spaces in the cooler and the condenser at the temperature of compression and expansion, respectively. The cooler dead space would be at a different temperature than the compression space as the gas is being cooled. At the same time, the ineffectiveness of the regenerator has been computed using a simple approach which does not take into account the complex nature of the processes occurring in the regenerator. In the present analysis, the cooler dead space temperature has been assumed to be the mean of the inlet and outlet temperatures. Miyabe's method⁴ has been used to calculate the ineffectiveness, which looks at the conditions existing in the regenerator. Again, Martini's approach² considers the loss analysis for average flow rates in the compression, the expansion and the regeneration processes, which would actually be sinusoidal. In the present work, the loss analysis considers the flow rates at different intervals for the existing pressures and temperatures. The cyclic analysis is thus more realistic in approach. The major assumption is the adiabatic nature of the compression process and the isothermal nature of the expansion process.

Assumptions

The important assumptions made are listed below:

- 1 the gas behaves as a perfect gas;
- 2 movements of the piston and displacer are sinusoidal;
- 3 the pressure in the system remains constant at any instant;
- 4 the compression process is adiabatic and the expansion process isothermal;
- 5 the cooler dead space temperature is at the mean of the inlet and outlet temperatures; and
- 6 the regenerator mass flow rate is the average of the mass flow rates of the compression and expansion spaces.

Pressure–volume variations

The volume variations for the expansion and compression spaces are given by the following expressions

$$V_E = V_{EC} + V_{EM} (1 - \cos \phi)/2 \quad (1)$$

$$V_C = V_{CC} + V_{EM} (1 + K + \cos \phi - K \times \cos (\phi - \alpha))/2 \quad (2)$$

The total mass of the working fluid is

$$M = M_C + M_{DC} + M_{RD} + M_{DCD} + M_E \quad (3)$$

Using perfect gas laws

$$P = \frac{MR}{\{(V_C/T_C) + (V_{DC}/T_{DC}) + (V_{RD}/T_{RD}) + (V_{DCD}/T_{DCD}) + (V_E/T_E)\}} \quad (4)$$

The magnitude of pressure, P , and volumes V_C and V_E and temperature T_C vary with crank angle, ϕ . The temperature T_E is assumed to remain constant. At the beginning, the cooler dead space temperature is assumed to be at compression space temperature. The regenerator temperature is assumed to be the logarithmic mean temperature of the two end temperatures.

Assuming the product of total mass in terms of moles of the gas, M , and the universal gas constant, R , (MR) to be unity, as the exact value of M is not known

$$P(1) = \frac{1}{\{V_C(1)/T_C(1) + V_{DC}/T_{DC} + V_{RD}/T_{RD} + V_{DCD}/T_{DCD} + V_E(1)/T_E\}} \quad (5)$$

For adiabatic compression, assuming $(\gamma - 1)/\gamma = E$

$$T_C(2) = T_C(1) \times (P(2)/P(1))^E \quad (6)$$

Substituting the values of $T_C(2)$, $V_C(2)$ and $V_E(2)$ in Equation (4), the equation then has only one variable, $P(2)$. The value of $P(2)$ could be obtained using the Newton-Raphson method. The value of $P(2)$ obtained is then used to calculate $P(3)$ and so on. In the same way, all the values of pressure and temperature are calculated for the complete cycle, depending on the interval chosen, ϕ . If ϕ is, for example, equal to 30, 13 points need to be calculated. The pressures and temperatures at the first and thirteenth points should match within the tolerance limit, otherwise the process of calculation restarts from the first point.

Mean pressure, P_m , would therefore be equal to

$$P_m = P_{TOTAL}/12 \quad (7)$$

The average existing pressure of the system, P_{avg} is known and the ratio of P_{avg} to P_m would give the correct value of MR . Previously, MR was assumed to be equal to unity. So, with the new values of MR , all the pressure values calculated earlier have to be corrected so that P_m matches P_{avg} .

Calculation of mass flow rates

The mass flow rate in the two working spaces is different because of the regenerator, cooler and condenser dead spaces. To calculate these mass flow rates, the variation of mass fraction of the gas inventory in each space for each interval is calculated

$$F_E(I) = P(I)V_E(I)/(MRT_E) \quad (8)$$

$$F_C(I) = P(I)V_C(I)/(MRT_C(I)) \quad (9)$$

Calculation of the mass flow rate involves conversion of

these fractions of masses existing in the working spaces to respective flow rates, by multiplying the fractions by the molecular weight of the working fluid and the speed

$$W_{ES}(I) = [F_E(I+1) - F_E(I)]M M_w N_U/(\phi/360) \quad (10)$$

$$W_{CS}(I) = [F_C(I+1) - F_C(I)]M M_w N_U/(\phi/360) \quad (11)$$

The function of the water cooler is to lower the temperature of the gas after compression to near ambient temperature. The water flow rates and temperature across the inlet and outlet of the water cooler are known. Using the heat balance equation, the decrease in temperature of the gas can be calculated. As the mass flow rate of gas in the cooler, $W_{CS}(I)$, is cyclic, the temperature change of water has to be cyclic. Assuming this, the effective average temperature difference can be computed, which should work out to be as specified or within the tolerance limits. After calculating the temperature changes of the gas due to the water cooler, the analysis restarts from the first pressure calculation to correct the assumption. The calculated temperature of gas, after the water cooler, is substituted in the equations to correct the cooler dead space temperature and the whole set of calculations is repeated. The analysis is repeated in this way until two successive mass flow rates do not vary beyond a specified limit.

Calculation of power input and refrigeration effect

The ideal power input to the system, C_p , and the refrigeration effect ideally available, Q_i , can be calculated once the pressure variations for the complete cycle are known. Therefore, C_p and Q_i can be given as

$$C_p(I) = \int P(I) dV_T(I) \quad (12)$$

$$Q_i(I) = \int P(I) dV_E(I) \quad (13)$$

$$V_T(I) = V_C(I) + V_D + V_E(I) \quad (14)$$

The integration can be done using the trapezoidal rule. The pressure taken for each interval is the average pressure of the interval. The algebraic sum of the product of pressure and volume difference for each interval gives the total C_p and Q_i .

Loss analysis

The loss analysis of the cryocooler is very important and demonstrates its influence on the efficiency and performance of the cryocooler. There are various losses in the system causing the net power supply to increase and the net refrigeration available to decrease.

Power requirement

The power requirement increases due to: 1, pressure drop because of flow friction in the cooler, the regenerator and the condenser; and 2, mechanical losses. Calculation of pressure drop in the cooler, the condenser and the regenerator can be done for the cyclic mass flow rates $W_{CS}(I)$, $W_{ES}(I)$ and $W_{RS}(I)$, respectively.

The friction factor is calculated from standard formulae available in the literature² for the existing conditions. The total pressure drop for the complete cycle can be

calculated as

$$C_{PL, total} = C_{PL, cooler} + C_{PL, reg} + C_{PL, cond}$$

This power loss is added to the ideally required power input. The mechanical efficiency takes various transmission losses into consideration.

Refrigeration capacity

Losses resulting in a reduction of refrigeration capacity are due to: 1, regenerator ineffectiveness; 2, shuttle heat conduction; 3, temperature swing; 4, pumping action; 5, instantaneous pressure drop; and 6, conduction through various solid parts.

Loss due to ineffectiveness of regenerator

The loss due to regenerator ineffectiveness is one of the major losses. Because of the ineffectiveness of the regenerator, the gas is cooled from $T_C(I)$ up to $(T_E + \Delta T)$ instead of T_E . A part of the refrigeration effect, therefore, is lost. To calculate this loss on a cyclic basis the effectiveness is calculated for each flow rate in the regenerator. The calculation of regenerator effectiveness is done using Miyabe's method⁴. The loss, $Q_R(I)$, for the I th interval is given as

$$Q_R(I) = W_{RS}(I) \times C_v \times (T_C(I) - T_E) \times (1 - E) \times (\text{interval time}) \quad (15)$$

The temperature difference $(T_C(I) - T_E)$ varies with each mass flow rate, $W_{RS}(I)$ (for the I th interval), and therefore with the effectiveness, E . The loss in refrigeration effect is calculated when the gas is moving up through the regenerator. This is taken care of by the sign convention of the mass flow rate, $W_{RS}(I)$.

The cumulative value of $Q_R(I)$ gives the total loss due to the ineffectiveness of the regenerator. The loss varies with different mesh structures used in the regenerator and also with the properties of the mesh materials.

Loss due to shuttle heat conduction

Longworth and Zimmermann⁵ have studied this loss in detail. The displacer absorbs heat at the hot end and gives it out at the cold end during its stroke. Shuttle heat conduction depends on the area involved, the thickness of the gap between the displacer and the outside wall, C_C , and the temperature gradient across the displacer. The heat transferred per half cycle time, t , can be given as

$$Q = K_g A (T_C(I) - T_E) t / C_C \quad (16)$$

where A is the surface area of the displacer.

The rate at which heat is transferred from the hot end of the displacer to the cold end depends on: 1, heat transfer between the displacer and the wall per cycle, Q ; 2, distance through which average energy is transported during each cycle, S_D ; 3, cycle rate, N_U ; and 4, distance between the hot and cold ends, L_D . Therefore, the loss is given as

$$Q_S = Q S_D N_U / L_D \quad (17)$$

Depending on the interval, the cycle period has to be identified when the loss would take place. The loss calculation is done for each interval.

Temperature swing loss

This loss accounts for the temperature changes in the matrix of the regenerator during the cycle. It is the heat taken up by the matrix due to its finite heat capacity. The drop in regenerator matrix temperature, all along the line, due to a single flow of gas in the expansion space, as given by Martini², is

$$D_{RMT}(I) = W_{RS}(I) \times C_v \times (T_C(I) - T_E)/(N_U M_{MX} C_{PM}) \times (\text{interval time}) \quad (18)$$

The temperature swing loss, therefore, is equal to

$$Q_{TS}(I) = W_{RS}(I) \times C_v \times D_{RMT}(I)/2 \times (\text{interval time}) \quad (19)$$

The loss is calculated when the gas moves up through the regenerator during the cycle.

Pumping loss

As the cooler is pressurized and depressurized, the gas present in the gap between the displacer and the wall flows into and out of this gap. Therefore, at the cold end, some of the refrigeration effect available is taken up by this gas, as given by Martini²

$$Q_{PU} = \left(\frac{\pi D_P \times 10^{+4}}{K_g} \right)^{0.6} \times \left(\frac{2L_D(T_C(I) - T_E) \times 10^{+2}}{1.5} \right) \times \left(\frac{(P_{MAX} - P_{MIN}) \times 10^{-1} N_U C_p 2 M_w}{(T_C(I) + T_E)R} \right)^{1.6} \times (C_C \times 10^{+2})^{2.6} \quad (20)$$

The loss is again calculated for each interval and the total gives the net loss during the complete cycle.

P-V loss due to pressure drop

Due to pressure drop in the cooler, the regenerator and the condenser, the expansion space pressure is always less than that of the compression space. The pressure in the expansion space would, therefore, be

$$P_E(I) = P(I) - (\text{total pressure drop})$$

In this way, all the values of $P_E(I)$ in the cycle are calculated. This reduces the refrigeration effect available from the system. The refrigeration effect, therefore, is given by

$$Q_{IP} = \int P_E(I) dV_E(I) \quad (21)$$

Again, the integration is carried out for small intervals of the cycle. The term $(Q_I - Q_{IP})$ gives the loss.

Loss due to conduction through solid members

The loss due to conduction continues independent of machine speed. It is the heat transferred through the different solid members between the hot and cold portions of the machine. It involves loss due to conduction

through: 1, displacer material; 2, regenerator outer and inner rings; and 3, regenerator matrix material. The losses are calculated from the basic equations in a cyclic manner.

Results and discussion

PPG-102

The present analysis was applied to PPG-102. Walker *et al.*³ applied the isothermal analysis to the same machine. The basic figures required are shown in *Figures 1–8*. The required data for the analysis are taken from Walker *et al.*³. *Tables 1* and *2* give a comparison of the power requirement and refrigeration effect obtained by Walker *et al.*³ and in the present analysis, respectively. *Table 3* gives a comparison of the overall performances of the machine obtained in both analyses. The mechanical efficiency of the compressor is assumed to be 70%.

The comparison shows that the present work is in better agreement with the actual results than Walker's

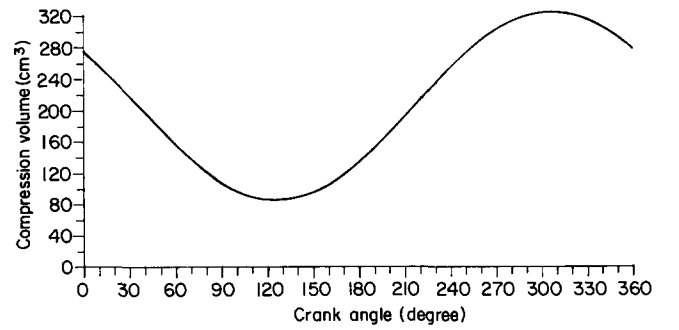


Figure 1 Compression volume variation

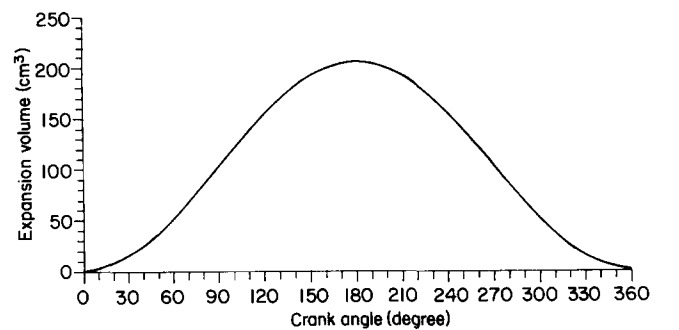


Figure 2 Expansion volume variation

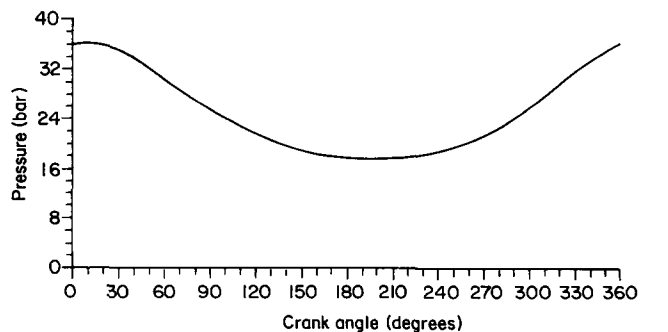


Figure 3 Pressure variation

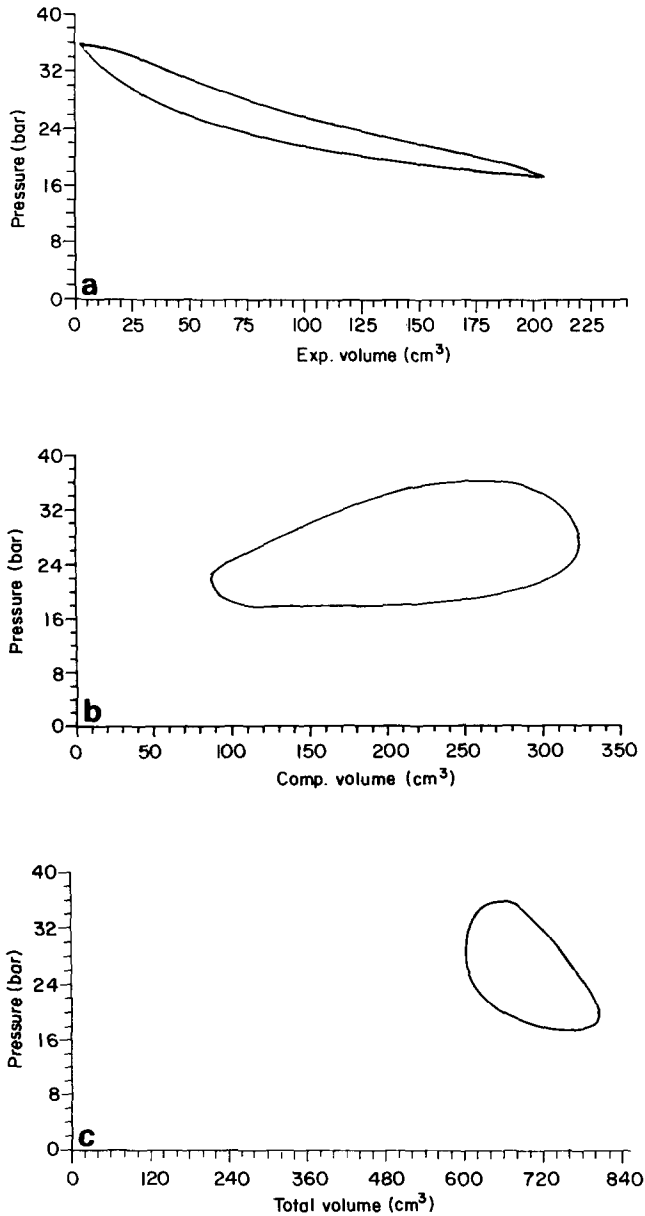


Figure 4 P-V diagrams for: (a) expansion volume; (b) compression volume; and (c) total volume

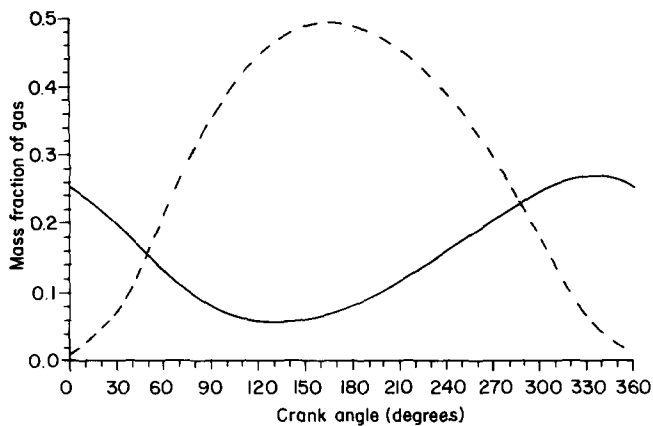


Figure 5 Gas flow distribution. ---, Expansion space; —, compression space

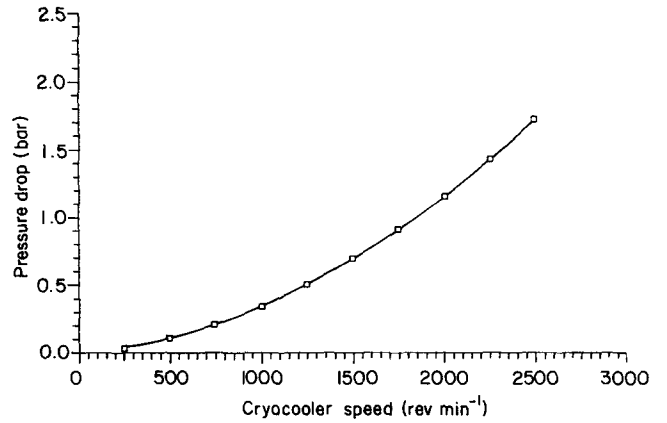


Figure 6 Pressure drop against speed (mean pressure 25 bar)

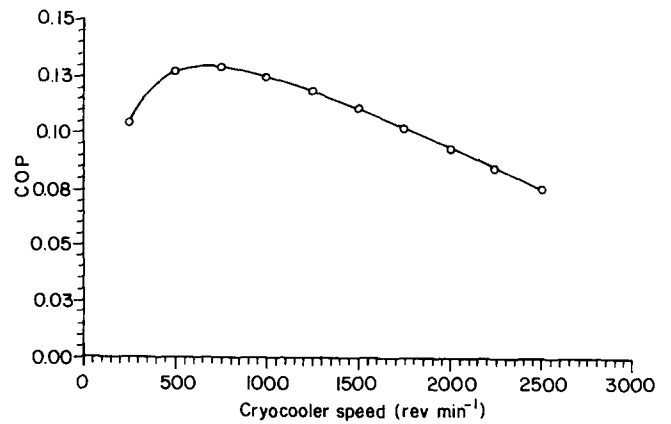


Figure 7 COP map against speed (mean pressure 25 bar)

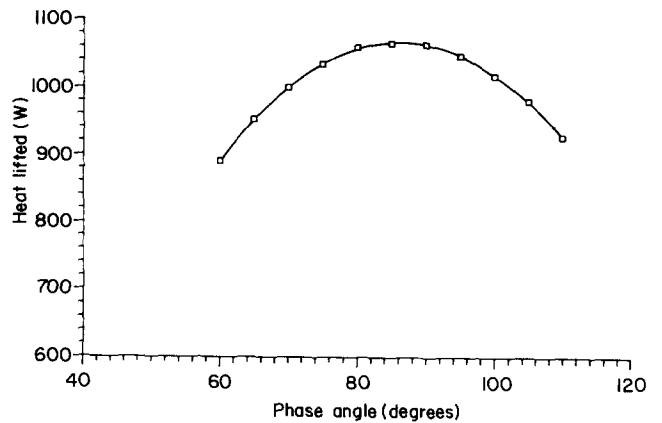


Figure 8 Effect of phase angle on heat lifted (mean pressure 25 bar)

results³. Figure 11a shows that the optimum performance of machine PPG-102, as indicated by COP, is obtained at a phase angle of 72°, as indicated by the present analysis. Walker's results³ do not show this. Also, Figure 7 shows the variation of COP against speed for PPG-102. The variation given by Walker *et al.*³ shows a sinusoidal type curve which does not match the given set of data. Figure 11b shows a comparison of the curves obtained for the variation of COP against speed by Walker *et al.*³ and in the present analysis. The curves obtained by Walker *et al.*³ for a mean pressure of 20 bar* show a very different

* 1 bar = 10⁵ Pa

Table 1 Comparison of power requirements for PPG-102 from Walker *et al.*³ and the present analysis

	Results from Walker <i>et al.</i> ³ (W)	Present results (W)
Basic power	4920.52	5541.04
Condenser flow loss	381.02	287.73
Regenerator flow loss	312.88	434.03
Cooler flow loss	117.31	81.04
Net power	5731.81	6343.84
Mechanical loss	2456.49	2718.78
Actual power	8188.29	9062.63

Table 2 Comparison of refrigeration available for PPG-102 from Walker *et al.*³ and the present analysis

	Results from Walker <i>et al.</i> ³ (W)	Present results (W)
Basic refrigeration	1379.23	1567.67
Regenerator loss	171.41	188.45
Shuttle	57.07	66.44
Pumping	103.03	113.29
Temperature swing	110.97	88.75
<i>P-V</i> loss due to pressure drop	Not considered	89.94
Conduction	3.20	3.20
Net capacity	933.51	1017.74

Table 3 Comparison of overall performance predictions

	Actual results ³	Results from Walker <i>et al.</i> ³	Present results
Power input (W)	9000	8188.29	9062.63
Net refrigeration (W)	1000	933.51	1017.75
COP	0.111	0.114	0.1123

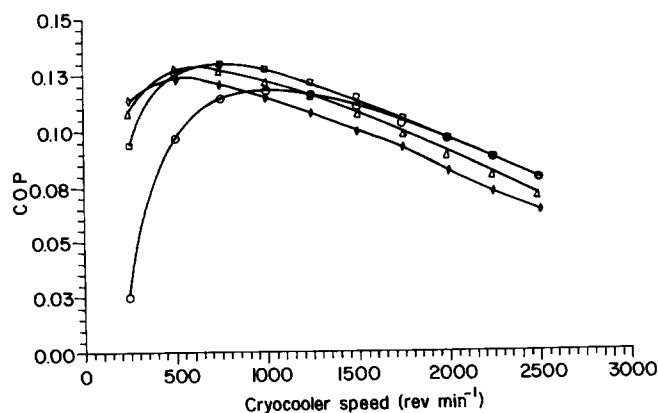


Figure 9 COP map against speed. Mean pressure: ○, 10 bar; □, 20 bar; △, 30 bar; ◇, 40 bar

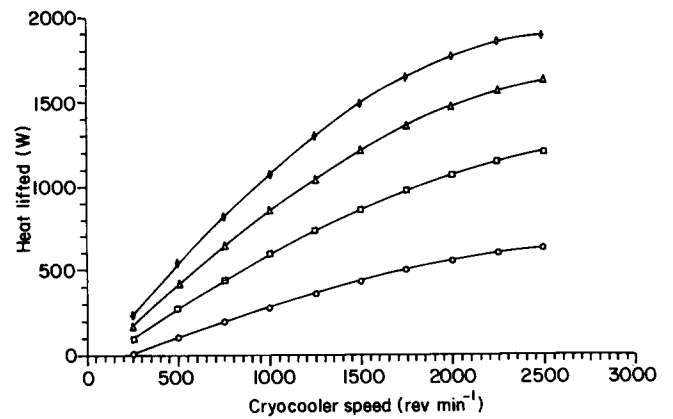


Figure 10 Heat map against speed. Mean pressure: ○, 10 bar; □, 20 bar; △, 30 bar; ◇, 40 bar

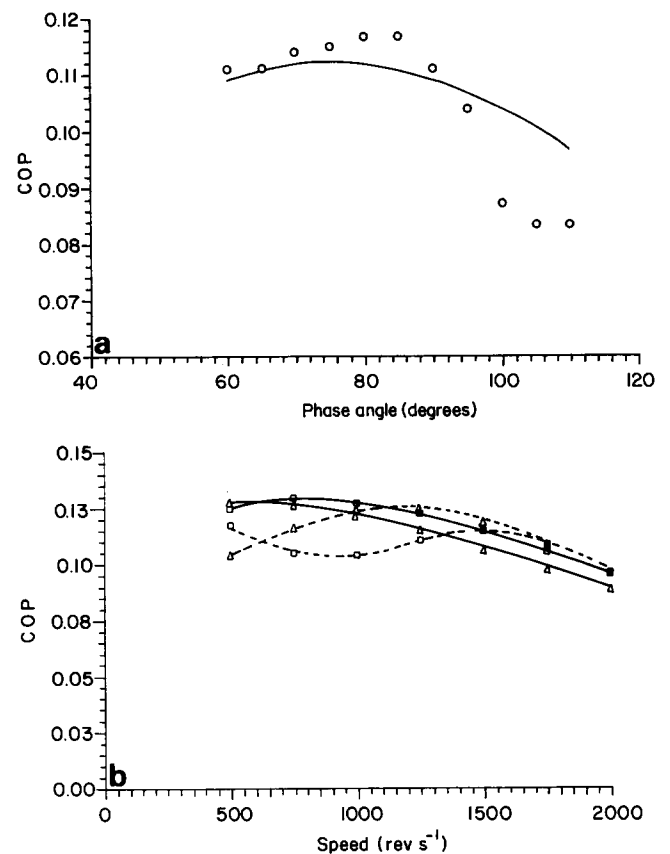


Figure 11 Comparison of present work with results from Walker *et al.*³. (a) COP versus phase angle: —, present results; ○, results from Walker *et al.*³. (b) COP versus speed: —, present results; ---, results from Walker *et al.*³. Mean pressure: □, 20 bar; △, 30 bar

pattern to those from the present analysis. *Figure 9* shows that the curves obtained for the variation of COP against speed for mean pressures of 10, 20, 30 and 40 bar follow a regular pattern with a single maximum in the normal operating speed range. As the mean pressure is increased, the maximum moves towards the left, due to higher overall losses at higher speeds. *Figure 10* gives the variation of net refrigeration effect against speed for mean pressures of 10, 20, 30 and 40 bar.

Table 4 Results for PLN-106^a

Power requirement (W)		Refrigeration available (W)	
Basic power	6992.74	Basic refrigeration	2010.80
Condenser flow loss	5.08	Regenerator loss	608.44
Regenerator flow loss	120.98	Shuttle	28.35
Cooler flow loss	70.27	Pumping	91.74
Net power	7189.07	Temperature swing	460.70
Mechanical loss	1797.26	<i>P-V</i> loss due to pressure drop	13.02
Actual power	8986.34	Conduction	20.72
Actual COP	0.0876	Net capacity	787.80

^a Specifications of PLN-106 (Philips, Holland): capacity of machine, 6–6.5 dm³ h⁻¹ liquid nitrogen; working fluid, hydrogen; mean pressure, 25 bar; speed, 1450 rev min⁻¹; cooling water flow rate, 0.75 m³ h⁻¹; assumed compressor mechanical efficiency, 80%

Table 5 Results for PLN-108S^a

Power requirement (W)		Refrigeration available (W)	
Basic power	7027.99	Basic refrigeration	2085.78
Condenser flow loss	6.81	Regenerator loss	536.48
Regenerator flow loss	65.34	Shuttle	26.65
Cooler flow loss	78.64	Pumping	93.29
Net power	7178.78	Temperature swing	413.85
Mechanical loss	1794.69	<i>P-V</i> loss due to pressure drop	7.49
Actual power	8973.49	Conduction	41.38
Actual COP	0.1077	Net capacity	966.60

^a Specifications of PLN-108S (Philips, Holland): capacity of machine, 8 dm³ h⁻¹ liquid nitrogen; working fluid, hydrogen; mean pressure, 30 bar; speed, 1450 rev min⁻¹; cooling water flow rate, 0.75 m³ h⁻¹; assumed compressor mechanical efficiency, 80%

PLN-106, PLN-108S and 3Mφ-1000

The analysis has been applied to different machines. The final results are given in *Tables 4, 5* and *6*. The specifications of the machines are given as footnotes to the respective tables.

The analytical results, given above, are calculated at the expansion space temperature of 77.12 K, while the

Table 6 Results for 3Mφ-1000^a

Power requirement (W)		Refrigeration available (W)	
Basic power	10628.85	Basic refrigeration	2980.17
Condenser flow loss	5.47	Regenerator loss	856.28
Regenerator flow loss	169.70	Shuttle	29.24
Cooler flow loss	160.49	Pumping	132.46
Net power	10964.51	Temperature swing	673.45
Mechanical loss	2741.12	<i>P-V</i> loss due to pressure drop	22.11
Actual power	13705.63	Conduction	21.16
Actual COP	0.0908	Net capacity	1245.43

^a Specifications of 3Mφ-1000 (USSR): capacity of machine, 10 dm³ h⁻¹ liquid nitrogen; working fluid, hydrogen; mean pressure, 25 bar; speed, 1460 rev min⁻¹; cooling water flow rate, 0.75 m³ h⁻¹; assumed compressor mechanical efficiency, 80%

compression space temperature varies according to the working fluid and the dead space geometry of the cryocooler.

Conclusions

The analysis gives a reasonable outline of the various losses and performances of the different machines. Consideration of the cyclic variation of mass flow rates and calculation of different losses for each interval of the cycle, show good agreement with the actual values. Also, the assumption of adiabatic compression and isothermal expansion makes the analysis more realistic.

References

- 1 Schmidt, G. Theorie der lehmanischen calorischen maschinen *Z Verh dt Ing* (1871) 15
- 2 Martini, W. Stirling engine design manual, NASA report, National Technical Information Services, US Department of Commerce, Springfield, USA (1978)
- 3 Walker, G., Weiss, M., Fauvel R. and Reader, G. Microcomputer simulation of Stirling cryocoolers *Cryogenics* 29 846–849
- 4 Miyabe, H., Takahashi, S. and Hamaguchi, K. An approach to the design of Stirling engine regenerator matrix using packs of wire gauges *Proc 17th IECEC IEEE*, New York, USA (1982) 1833–1844
- 5 Longworth, R. C. and Zimmermann, F. J. Shuttle heat transfer *Adv Cryog Eng* (1970) 16 342–351